Synthesis, Crystal Structure and DFT Calculation of 2-Methoxyimino Phenylacetate Derivatives Containing 1,3,4-Oxadiazole Ring①

REN Hui-Dong[a] LI Kang-Ming[a] YI Yang-Jie[a]
WANG Man[a] YE Jiao[a②] HU Ai-Xi[a②]
CHEN Yun[a] OU Xiao-Ming[b] LI Jian-Ming[b]

[a] (*College of Chemistry and Chemical Engineering, Hunan University, Changsha* 410082, *China*)
[b] (*National Pesticide Creation Engineering Technology Research Center, Hunan Research Institute of Chemical Industry Co., Ltd., Changsha* 410007, *China*)

ABSTRACT Four novel 2-methoxyimino phenylacetate derivatives containing 1,3,4-oxadiazole ring were designed and synthesized from the key intermediate of *Trifloxystrobin* or *Azoxystrobin* via intermediate derivatization and active structure splicing. The chemical structures of the target compounds were confirmed by ^{1}H NMR, ^{13}C NMR and elemental analysis. The crystal structure of methyl (E)-2-(methoxyimino)-2-(2-(((5-((4-methoxyphenoxy)methyl)-1,3,4-oxadiazol-2-yl)thio)methyl)phenyl)acetate (**A1**) was determined by single-crystal X-ray diffraction. Compound **A1** belongs to triclinic system, space group $P\bar{1}$ with two molecules in each unit cell. The benzene ring plane C(2)–C(3)–C(4)–C(5)–C(6)–C(7) and oxazole ring plane are nearly parallel with the dihedral angle of 6.4°. The benzene ring plane C(12)–C(13)–C(14)–C(15)–C(16)–C(17) and oxazole ring plane are not perpendicular with the dihedral angle of 49.4°. The crystal of compound **A1** is stabilized by π-π stacking interactions. The fungicidal activities of the target compounds against four plant pathogenic fungi in vitro were tested, and some of them had good activities. The DFT calculation was carried out to study the structure-activity relationship of the title derivatives using Gasian 09 and Multiwfn 3.6.

Keywords: 2-methoxyimino phenylacetate derivatives, synthesis, crystal structure, fungicidal activities, DFT calculation; DOI: 10.14102/j.cnki.0254-5861.2011-3292

1 INTRODUCTION

The research of heterocyclic compounds is the trend of modern pesticide development. As an important member of nitrogen-containing heterocyclic compounds, oxadiazole derivatives have a wide range of applications in chemistry and biology. They not only have excellent insecticidal[1-3], bactericidal[4-6], herbicidal[7-10], anticancer[11] and anti-inflammatory[12] activities, but also can be used as electron transport materials[13, 14]. In recent years, it has been found that phenoxy-1,3,4-oxadiazole ring is a mature bioactive fragment with good antibacterial activity and bactericidal universal type[15-19].

In addition, 2-methoxyiminobenzoacetate fungicides are one of the main fungicides at present. Among them, *Trifloxystrobin* and *Azoxystrobin* are widely used in fruits and vegetables because of their unique mechanism of action, high efficiency, broad spectrum and low toxicity. Therefore, the development of *Trifloxystrobin* or *Azoxystrobin* analogues with independent intellectual property rights will have a large market space in the future.

Recently, we have designed and synthesized four novel 2-methoxyimino-phenylacetate derivatives (**A**) containing 1,3,4-oxadiazole ring by introducing the bioactive fragment of 1,3,4-oxadiazole ring into the side chain of compound (**B**), which is the key intermediate for the synthesis of *Trifloxystrobin* or *Azoxystrobin*. The chemical structures of the target compounds were confirmed by ^{1}H NMR, ^{13}C NMR and elemental analysis. The crystal structure of methyl (E)-2-(methoxyimino)-2-(2-(((5-((4-methoxyphenoxy)me-

Received 2 June 2021; accepted 6 September 2021 (**CCDC 2064038**)

① This project was supported by the National Key R & D Program of China (No. 2016YFD0300708)

② Corresponding authors. E-mails: yejiao@hnu.edu.cn and axhu@hnu.edu.cn

thyl)-1,3,4-oxadiazol-2-yl)thio)methyl)phenyl) acetate (**A1**) was determined by single-crystal X-ray diffraction. In addition, the fungicidal activities of the target derivatives against four phytopathogenic fungi were tested, and the structure-activity relationship was analyzed combining with the DFT calculation, which established a guiding significance for subsequent development. The synthetic route of the title derivatives is depicted in Scheme 1.

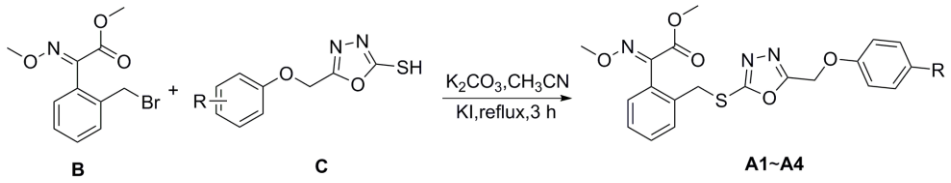

Scheme 1. Synthetic route of 2-methoxyimino phenylacetate derivatives containing 1,3,4-oxadiazole ring

2 EXPERIMENTAL

2. 1 Materials and methods

All the reagents and solvents were purchased from commercial sources and used without further purification. Melting points (℃) were determined on an X-4 electro-thermal digital melting point apparatus and uncorrected. ^{1}H NMR and ^{13}C NMR spectra were recorded on a Bruker advanced instrument with TMS as the internal standard at 400 MHz (chemical shifts (δ) in ppm). The Bruker AXS SMART 1000 CCD diffractometer was used for crystal structure determination. The VARIO EL III elemental analyzer provides the elemental analysis data of compounds. The data of fungicidal activity in vitro provided by Hunan Research Institute of Chemical Industry Co, Ltd and National pesticide Creation Engineering Technology Research. The course of the reactions was monitored by TLC, and analytical TLC was performed on silica gel GF254.

2. 2 General procedure

2. 2. 1 Synthesis of intermediates B and C

Intermediate **B** was synthesized according to the method in reference[20-22]. *O*-methyl acetophenone was selected as raw material, and **B** was prepared via oxidation, esterification, oximation and bromination with overall yield of 55.7%.

Intermediate **C** was synthesized according to the method in reference[23]. The corresponding substituted phenol was selected as the raw material, which reacted with chloroacetic acid, then esterified, and reacted with hydrazine hydrate to obtain corresponding aryloxyacetylhydrazine, and finally cyclized with carbon disulfide to obtain **C**.

2. 2. 2 Syntheses of the target compounds A1～A4

1.0 mmol compound **C**, 1.1 mmol potassium carbonate, 5 mL acetonitrile, 0.6 mmol potassium iodide and 1.05 mmol compound **B** were added in batches under room temperature with stirring, and then the reaction mixture was heated to reflux for 3 hours. Compounds **A1**～**A4** were obtained by column chromatography using petroleum ether/ethyl acetate (v/v = 10:1) as eluent.

Methyl (E)-2-(methoxyimino)-2-(2-(((5-((4-methoxy-phenoxy)methyl)-1,3,4-oxadiazol-2-yl)thio)methyl)phenyl) acetate (**A1**). Yield: 58.3%, white solid, m.p. 73～75 ℃. ^{1}H NMR (400 MHz, $CDCl_3$) δ: 7.60～7.12 (m, 4H, PhH), 6.93 (d, J = 9.1 Hz, 2H, PhH 2,6-H), 6.83 (d, J = 9.1 Hz, 2H, PhH 3,5-H), 5.14 (s, 2H, OCH_2), 4.35 (s, 2H, SCH_2), 4.07 (s, 3H, $NOCH_3$), 3.89 (s, 3H, $COOCH_3$), 3.76 (s, 3H, OCH_3); ^{13}C NMR (100 MHz, $CDCl_3$) δ: 165.57, 163.60, 163.21, 154.93, 151.63, 149.02, 133.79, 130.58, 130.21, 129.86, 128.66, 128.13, 116.22, 114.81, 63.92, 60.76, 55.69, 53.16, 34.68. Anal. Calcd. (%) for $C_{21}H_{21}N_3O_6S$: C, 56.88; H, 4.77; N, 9.48. Found (%): C, 56.88; H, 4.78; N, 9.46.

Methyl (E)-2-(methoxyimino)-2-(2-(((5-((*p*-tolyloxy)me-thyl)-1,3,4-oxadiazol-2-yl)thio)methyl)phenyl)acetate (**A2**). Yield: 74.0%, white solid, m.p. 82～84 ℃. ^{1}H NMR (400 MHz, $CDCl_3$) δ: 7.59～7.15 (m, 4H, PhH), 7.10 (d, J = 8.2 Hz, 2H, C_6H_2 3,5-H), 6.88(d, J = 8.2 Hz, 2H, C_6H_2 2,6-H), 5.17(s, 2H, OCH_2), 4.35(s, 2H, SCH_2), 4.07 (s, 3H, $NOCH_3$), 3.89(s, 3H, OCH_3), 2.29(s, 3H, CH_3). ^{13}C NMR (100 MHz, $CDCl_3$) δ: 165.58, 163.56, 163.22, 155.44, 149.02, 133.79, 131.62, 130.58, 130.21, 130.14, 129.86, 128.66, 128.13, 114.78, 63.92, 60.02, 53.17, 34.68, 20.50. Anal. Calcd. (%) for $C_{21}H_{21}N_3O_5S$: C, 59.02; H, 4.92; N, 9.84. Found (%): C, 58.98; H, 4.93; N, 9.86.

Methyl (E)-2-(2-(((5-((4-chlorophenoxy)methyl)-1,3,4-oxadiazol-2-yl)thio)methyl)phenyl)-2-(methoxyimino)acetate (**A3**). Yield: 58.3%, yellow solid, m.p. 92～94 ℃. ^{1}H NMR (400 MHz, $CDCl_3$) δ: 7.59～7.15(m, 4H, Ar–H), 7.26(d, J = 9.0 Hz, 2H, C_6H_4 3,5-2H), 6.92 (d, J = 9.0 Hz, 2H, C_6H_4 2,6-2H), 5.17 (s, 2H, OCH_2), 4.35 (s, 2H, SCH_2), 4.06 (s, 3H, CH_3), 3.88 (s, 3H, CH_3); ^{13}C NMR (100 MHz, $CDCl_3$) δ: 165.35, 164.12, 163.25, 150.67, 149.03, 134.67, 133.79, 130.74, 130.59, 130.22, 129.90, 128.76, 128.22, 127.42, 125.51, 124.99, 63.96, 53.20, 34.84, 20.37. Anal. Calcd. (%). for $C_{20}H_{19}N_3O_5S$: C, 58.10; H, 4.63; N, 10.16. Found: C, 58.08; H, 4.64; N, 10.17.

Methyl(E)-2-(methoxyimino)-2-(2-(((5-((4-nitrophenoxy)methyl)-1,3,4-oxadiazol-2-yl)thio)methyl)phenyl) acetate (**A4**). Yield: 73.9%, viscous liquid. ^{1}H NMR (400 MHz, $CDCl_3$) δ: 8.22 (d, J = 9.2 Hz, 2H, C_6H_4 3,5-H), 7.60～7.14(m, 4H, PhH), 7.09 (d, J = 9.2 Hz, 2H, C_6H_4 2,6-H), 5.30 (s, 2H, OCH_2), 4.35 (s, 2H, SCH_2), 4.06 (s, 3H, $NOCH_3$), 3.89 (s, 3H, OCH_3); ^{13}C NMR (100 MHz, $CDCl_3$) δ: 166.16, 163.21, 162.21, 162.05, 148.98, 142.64, 133.63, 130.58, 130.18, 129.87, 128.72, 128.22, 126.03, 114.92, 63.94, 59.92, 53.18, 34.73. Anal. Calcd. (%) for $C_{20}H_{19}N_3O_5S$: C, 58.10; H, 4.63; N, 10.16. Found: C, 58.08; H, 4.64; N, 10.17.

2. 3 X-ray structure determination

The representative compound **A1** was dissolved in EtOH and kept for self-volatilization. The colorless crystals suitable for X-ray structure determination were obtained after about 6 days with dimensions of 0.12mm × 0.11mm × 0.1mm. X-ray intensity data were measured on the BRUKER SMCRT 1000 CCD diffractometer, and collected at 273.15 K by using a graphite-monochromatic with Mo$K\alpha$ radiation (λ = 0.71073 Å) in an ω-ϕ scan mode. Out of the total 9597 reflections collected in the range of $2.36 \leqslant \theta \leqslant 28.33°$, 4931 were independent (R_{int} = 0.0361) and 283 were considered to be observed ($I > 2\sigma(I)$) and used in the succeeding refinement. Corrections for incident and empirical adsorption adjustment were applied with SADABS[24], and the structure was solved with SHELXS-97[25] and expanded by difference Fourier techniques. All non-hydrogen atoms were refined anisotropically and all H atoms were located at the theoretical positions. The structure was refined by full-matrix least-squares techniques on F^2 with SHELXL-97. The final refinement converged at R = 0.0669, wR = 0.1266 ($w = 1/[\sigma^2(F_o^2) + (0.0449P)^2 + 0.7314P]$, where $P = (F_o^2 + 2F_c^2)/3$), S = 1.038, $(\Delta\rho)_{max}$ = 0.814 and $(\Delta\rho)_{min}$ = –0.293 e/Å^3.

2. 4 Fungicidal bioassay in vitro

The fungicidal activities of compounds **A1**～**A4** have been determined using the mycelium growth rate method and *Phytophthora capsici* (PC), *Alternaria alternate* (AA), *Gibberella zeae* (GZ) and *Botrytis cinerea* (BC) were selected as fungicidal targets in vitro. According to NY/T1156.2-2006[26] as the biological activity test standard, the test compound was prepared into 500 mg/L drug solution, and 2 mL drug solution was added into 38 mL PDA to prepare the final concentration of 25 mg/L drug containing medium plate. Then about 6.5 mm mycelium was taken and transferred to the drug containing medium. After treatment, the drug containing medium was cultured in a constant temperature biochemical incubator at 28 ℃ for 96 hours, and the growth inhibition rate was calculated by measuring the diameter of the colony.

2. 5 DFT calculation

The ground state geometries of **A1**～**A4** were computed by using density functional theory (DFT) with Gaussian 09 package[27] and all the calculations were performed at the Becke-Lee-Parr hybrid exchange correlation three-parameter (B3LYP) functional[28] level with standard 6-31G(d, p)[29] basis set. Electrostatic potential (ESP) on molecular van der Waals surface was calculated by Multiwfn 3.6 based on B3LYP/6-31G (d, p) density[30, 31] and the surface area was plotted by VMD 1.9.3 program[32].

3 RESULTS AND DISCUSSION

3. 1 Synthesis and characterization

Intermediate **B** reacted with intermediate **C** via Williamson etherification to give **A1**～**A4** in 58.3%～74.0% yields and the structure of compounds was determined by ^{1}H NMR, ^{13}C NMR and elemental analysis.

From ^{1}H NMR data, the methyl peak on -OCH_3 is located at δ 3.88～3.90 ppm; The methyl peak of -$NOCH_3$ is found at δ 4.07～4.09 ppm; The methyl group on -SCH_2- appears at the δ 4.35～4.40 ppm and a single peak with a peak area of 2 near δ 5.20 ppm is assigned to -OCH_2-. It is consistent with the peak rule[33, 34].

In the ^{13}C NMR of the target compounds, there are four carbons in the high field, which exactly corresponds to the four high field alkyl carbons of the target compounds. There is a response at δ 160 ppm, which further confirms that there

is a carbonyl structure in the structure. The imine carbon (-C=N-) near δ 133.74 ppm further indicates that the structure contains oxime methyl ether structure. The peak positions of other carbons are consistent with the peak regularity.

The element analysis result of **A1**～**A4** is agreement with the calculated value.

3. 2 Crystal structure

Compound **A1** was selected as the representative of this kind of derivatives for crystal structure analysis. Some representative bond lengths and bond angles are listed in Table 1, and selected crystal torsion angles are listed in Table 2. The crystal structure and packing diagram of **A1** are illustrated in Figs. 1 and 2, respectively. Compound **A1** belongs to triclinic system, space group $P\bar{1}$, and each unit cell contains two molecules. The unit cell parameter is a = 7.6716(16) Å, α = 88.615(4) °, b = 8.3065(12) Å, β = 81.736(5) °, c = 17.482(4) Å, γ = 65.629(5) °, Z = 2, V = 1003.4(3) × 10^3 Å^3, D_c = 1.468 g/cm^3, F(000) = 464, μ = 0.207 mm^{-1} and 283 observable points ($I > 2\sigma(I)$). The final deviation factor of observable point finishing is R = 0.0669, wR = 0.1266, S = 1.038, $(\Delta\rho)_{max}$ = 0.814 and $(\Delta\rho)_{min}$ = –0.293 e/Å^3.

Table 1. Selected Bond Lengths (Å) and Bond Angles (°)

Bond	Dist.	Bond	Dist.	Bond	Dist.
S(1)–C(10)	1.732(3)	N(1)–N(2)	1.421(3)	N(3)–C(18)	1.292(2)
S(1)–C(11)	1.820(3)	N(1)–C(9)	1.279(3)	O(6)–C(21)	1.428(2)
O(1)–C(2)	1.372(3)	O(5)–C(19)	1.218(3)	O(1)–C(1)	1.424(3)
C(7)–C(2)	1.386(3)	O(2)–C(8)	1.411(3)	O(3)–C(10)	1.368(3)
O(6)–N(3)	1.396(3)	O(3)–C(9)	1.366(3)	O(6)–C(21)	1.428(2)
Angle	(°)	Angle	(°)	Angle	(°)
C(10)–S(1)–C(11)	97.1(1)	C(19)–O(4)–C(20)	114.8(2)	C(2)–O(1)–C(1)	117.0(2)
C(9)–O(3)–C(10)	101.5(2)	S(1)–C(11)–C(12)	110.4(2)	C(5)–O(2)–C(8)	116.9(2)
N(2)–C(10)–O(3)	113.6(2)	C(18)–N(3)–O(6)	110.9(2)	N(2)–C(10)–S(1)	130.0(2)
C(18)–N(3)–O(6)	110.9(2)	O(3)–C(10)–S(1)	116.4(2)	O(5)–C(19)–O(4)	123.5(2)
N(3)–C(18)–C(19)	112.4(2)	N(3)–O(6)–C(21)	108.2(2)	C(12)–C(11)–H(11)	109.6
C(6)–C(5)–O(2)	125.7(2)	N(3)–C(18)–C(17)	125.7(2)	N(1)–C(9)–C(8)	130.3(2)

Table 2. Selected Torsion Angles (Å)

Angle	(°)	Angle	(°)
C(21)–O(6)–N(3)–C(18)	–168.8(2)	C(16)–C(17)–C(18)–N(3)	–115.9(3)
C(11)–S(1)–C(10)–O(3)	173.6(2)	C(12)–C(17)–C(18)–N(3)	63.0(3)
C(5)–O(2)–C(8)–C(9)	–176.9(2)	N(3)–C(18)–C(19)–O(4)	165.4(2)
C(17)–C(18)–C(19)–O(5)	160.9(2)	N(3)–C(18)–C(19)–O(5)	–16.9(3)

As shown in Table 1, all of the bond angles and bond lengths are in normal ranges. The N(1)–C(9) (1.279(3) Å) and N(3)–C(18) (1.292(2) Å) of 1,3,4-oxadiazole ring were close to the normal C=N (1.27 Å)[35], while the O(5)–C(19) (1.218(3) Å) and O(3)–C(9) (1.366(3) Å) are shorter than the normal O(1)–C(1) (1.424(3) Å) because of the conjugation effect. The angle of C(10)–S(1)–C(11) is 97.1 ° due to the *S* atom belonging to sp^3 hybridization and containing two pairs of lone pairs of electrons. The torsion angle of C(21)–O(6)–N(3)–C(18) is –168.8(2) ° (Table 2), which means that the methoxyimino group is in *E*-type configuration.

As outlined in Fig. 1, there are three planes in the molecule. The benzene ring plane C(2)–C(3)–C(4)–C(5)–C(6)–C(7) and oxazole ring plane are nearly parallel with the dihedral angle of 6.4 °. The dihedral angle of benzene ring plane C(12)–C(13)–C(14)–C(15)–C(16)–C(17) and oxazole ring plane is 49.4 °, which indicated that the two planes are not perpendicular.

The cell packing diagram (Fig. 2) shows no hydrogen bonds in the unit cell. The crystal of compound **A1** is stabilized by π-π stacking interactions. The molecules are packed in a head-to-tail arrangement showing π-π stacking interactions. The distance between the centroid of the benzene ring plane C(2)–C(3)–C(4)–C(5)–C(6)–C(7) and the oxazole ring plane is 3.673 Å, and that from the centroid of the oxazole ring to the plane of the benzene ring plane C(2)–C(3)–C(4)–C(5)–C(6)–C(7) is 3.513 Å, with the angle between them to be 1.493 °. The values of the distance are also in accordance with π-π stacking[36].

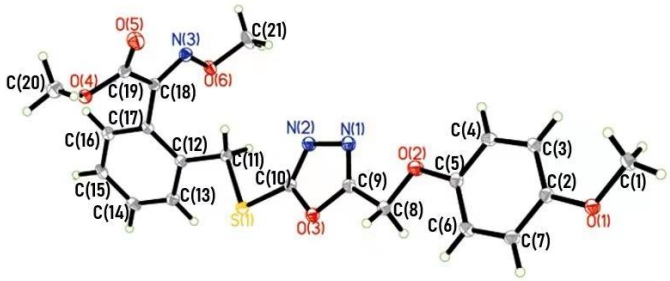

Fig. 1. Crystal structure of compound A1 with atom labels

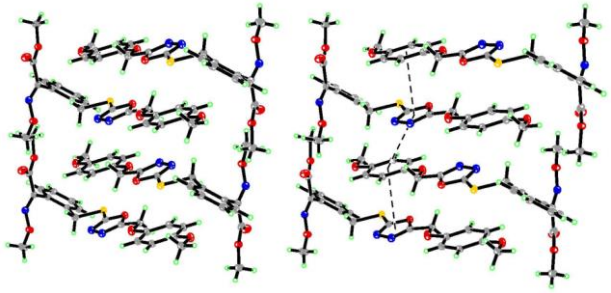

Fig. 2. Unit cell packing diagram of compounds A1

3. 3 Fungicidal activity

In this experiment, the key intermediate of *Trifloxystrobin* was used to design new compounds. In order to investigate the effect of the introduced fragment on fungicidal activity, *Trifloxystrobin* was selected as the positive control. The fungicidal activities of **A1**～**A4** are listed in Table 3.

Compounds **A1** ～ **A4** exhibited weak to moderate inhibitory activity against the four plant fungus. As the electron-withdrawing ability of the substituents (from **A1** to **A4**) increases, the inhibitory activity against *P. capsici* increases significantly, and **A4** (R = 4-NO_2) is the most potent compound; While the same regular is exhibited for *G. zeae*, the electron withdrawing substituent (**A3** R = 4-Cl; **A4** R = 4-NO_2) has better fungicidal activity; For *A. alternata* and *B. cinerea*, however, the inhibitory activity is better when R is weak electron donating substituents (**A2** R = 4-CH_3). **A1** with stronger electron donating substituent (4-OCH_3) exhibits very weak fungicidal activity against all the four fungus.

Table 3. Chemical Structures and Antifungal Activities in Vitro of the Target Compounds

Compd.	R	Inhibition rate (%)			
		P. capsici	*A. alternata*	*G. zeae*	*B. cinerea*
A1	4-OCH_3	2.00	12.94	9.52	22.00
A2	4-CH_3	19.07	35.40	46.07	41.01
A3	4-Cl	22.18	35.40	50.56	24.16
A4	4-NO_2	32.00	22.35	50.00	22.00
Trifloxystrobin		33.30	—	53.30	32.80

3. 4 DFT calculation

According to the frontier sub-orbital theory, the highest occupied molecular orbital (HOMO) and the lowest occupied molecular orbital (LUMO) can give priority to and receive electrons respectively[37]. These two molecular orbitals are important quantum chemical parameters that can affect biological activity[38, 39]. Density functional theory is adopted. The theoretical Becke three-parameter mixed functional method (B3LYP) calculates the FMO energy data for compounds **A1**～**A4** and the schematic diagram of the energy level orbital and the energy level difference are shown in Fig. 3.

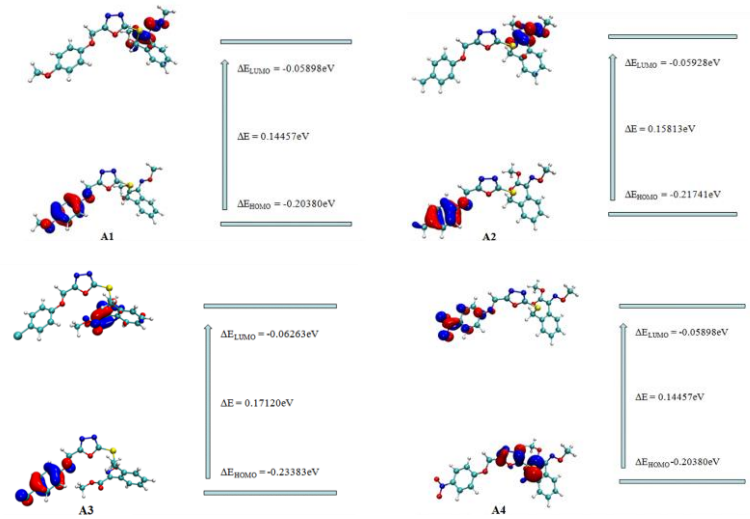

Fig. 3. LUMO, HOMO and energy gap of compound A1～A4

According to the FMO energy data and the diagram of energy level orbital and energy level difference, compounds **A1** and **A2** have the same characteristics. LUMO orbitals are mainly distributed in methyl methoxyiminoacetate, while HOMO orbitals are mainly distributed in the benzene ring connected with oxazole ring through -CH_2O-, which is caused by the fact that the substituents are electron donating groups.

In contrast, compounds **A3** and **A4** have different electron withdrawing groups. The LUMO orbitals of **A3** are mainly concentrated in the methyl methoxyiminophenyl acetate part, while the HOMO orbitals are concentrated in the oxazole ring connected through -CH_2O-. The LUMO orbital of compound **A4** is mainly distributed on the benzene ring connected to the oxazole ring through -CH_2O-, and the HOMO orbital is concentrated on -SCH_2- connected to the oxazole ring.

The molecular van der Waals surface electrostatic potential (ESP) is the key to studying and predicting the interaction between molecules[40, 41]. Fig. 4 shows the surface electrostatic potential of molecular van der Waals calculated by Multiwn 3.6, and the electrostatic potential diagram drawn by VMD program. The molecular size, structure and charge density of **A1**～**A4** are also obtained.

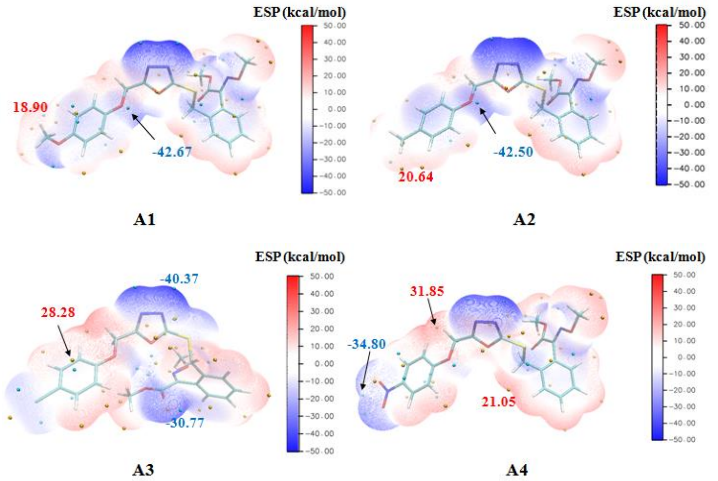

Fig. 4. ESP-mapped molecular vdW surface of compound A1～A4

It can be seen from the electrostatic potential diagram that the negative charge of **A1** and **A2** is mainly concentrated on the *O* atom of the oxazole ring and the benzene ring -OCH_2-, and the positive charge is concentrated around the electron-donating substituent. The negative charge of **A3** is mainly concentrated on the N–N bond of oxazole ring and methyl methoxyiminoacetate, while the positive charge is concentrated on the plane of C(2)–C(3)–C(4)–C(5)–C(6)–C(7) benzene ring. The negative charge of **A4** is concentrated on the two *O* atoms of NO_2, and the positive charge is

concentrated on the link bond -OCH_2-.

Combined with the analysis of fungicidal activity data, it is found that for *P. capsici*, *A. alternate*, *G. zeae* and *B. cinerea* the spatial structure of substituents has the greatest influence on the activity, and the longer substituents were not conducive to the inhibitory activity against the four fungi. For *P. capsici*, the more negative charge concentrated on the substituent, the better the fungicidal activity; For *B. cinerea*, the more negative charge concentrated on the link -OCH_2-, the better the fungicidal activity. This provides a guiding significance for the subsequent development of methyl methoxyiminophenyl acetate derivatives with stronger fungicidal activity.

4 CONCLUSION

In this paper, two broad-spectrum fungicidal active groups of 2-methoxyiminophenylacetate and oxadiazole ring were spliced together, and four 2-methoxy ethylene groups containing 1,3,4-oxadiazole ring were designed and synthesized, yielding 58.3%～74.0%. The structure of the target compound was characterized, and the single-crystal X-ray diffraction analysis of compound **A1** showed that it belongs to the triclinic crystal system with space group $P\bar{1}$. The C(18)=N(3) in the molecule is in the *E*-type configuration, and each unit cell contains two molecules, and the entire crystal is stabilized by π-π stacking. The in vitro fungicidal activity test found that at a concentration of 25 mg/L, the title compounds have a certain inhibitory effect on *P. capsici*, *A. alternate*, *G. zeae* and *B.cinerea*. By combining the fungicidal activity data with the DFT calculation results of the configuration of compounds **A1** ～ **A4**, it has guiding significance for the research of new 2-methoxyimino-phenylacetate fungicides.

REFERENCES

(1) Guo, Y.; Qu, L. L.; Wang, X. G.; Huang, M. X.; Jia, L.; Zhang, Y. B. Iodine-catalyzed oxidative cyclisation for the synthesis of sarisan analogues containing 1,3,4-oxadiazole as insecticidal agents. *RSC. Adv.* **2016**, 6, 93505–93510.

(2) Li, X. W.; He, D. H. Synthesis, crystal structure and biological activity of 2-(anthracen-9-yl)-5-*p*-tolyl-1,3,4-oxadiazole. *Chin. J. Struct. Chem.* **2012**, 31, 367–372.

(3) Zhou, Q.; Zheng, D. D.; Shi, Y. J.; Yao, W.; Qian, H. W.; Ding, Y.; Wei, Z. H.; Shen, A. B.; Feng, X.; Shi, J.; Dai, H. Synthesis and insecticidal activities of novel pyrazole oxime ethers containing an oxazole moiety. *Chin. J. Org. Chem.* **2018**, 38, 3318–3325.

(4) Kapoor, A.; Dhiman, N. Synthesis and evaluation of 2-aryl substituted benzimidazole derivatives bearing 1,3,4-oxadiazole nucleus for antimicrobial activity. *Der Pharmacia Sinica* **2019**, 8, 97–104.

(5) Sun, G. X.; Shi, Y. X.; Zhai, Z. W.; Sun, Z. H.; Weng, J. Q.; Tan, C. X.; Liu, X. H.; Li, B. J. Synthesis, crystal structure and antifungal activity of 2-((2-fluorobenzyl)thio)-5-(pyridin-4-yl)-1,3,4-oxadiazole. *Chin. J. Struct. Chem.* **2016**, 35, 1855–1859.

(6) Liu, J. C.; Wang, W. D.; He, H. W. Synthesis and fungicidal activity of 2,5-substituted-1,3,4-oxadiazole derivatives. *Chin. J. Org. Chem.* **2014**, 34, 1447–1451.

(7) Kalhor, M.; Dadras, A. Synthesis, characterization and herbicidal activities of new 1,3,4-oxadiazoles, 1,3,4-thiadiazoles and 1,2,4-triazoles derivatives bearing (R)-5-chloro-3-fluoro-2-phenoxypyridine. *J. Heterocyclic Chem.* **2013**, 50, 220–224.

(8) Shi, Y. J.; Li, Y.; Fang, Y.; Chen, J.; Ye, L. Y.; Ge, S. S.; Dai, H. Synthesis and biological activity of novel cyanoacrylate containing 1,3,4-oxadiazole moiety. *Chin. J. Org. Chem.* **2016**, 36, 2472–2478.

(9) Mo, Q. J.; Duan, W. G.; Li, X. R.; Huang, D. P.; Luo, Z. J. Synthesis and herbicidal activity of 2-substituted amino-5-dehydroabietyl-1,3,4-oxadiazole derivatives. *Chin. J. Org. Chem.* **2011**, 31, 1114–1121.

(10) Huang, T. H.; Chen, H.; Chen, J.; Zhang, A. D. Syntheses, crystal structures, and biological activities of two 5-pyrimidinyl-1,2,4-oxadiazoles. *Chin. J. Struct. Chem.* **2014**, 33, 1455–1459.

(11) Mochona, B.; Mazzio, E.; Gangapurum, M.; Mateeva, N.; Redda, K. K. Synthesis of some benzimidazole derivatives bearing 1,3,4-oxadiazole moiety as anticancer agents. *Chem. Sci. Trans*. **2015**, 4, 534–540.

(12) Zheng, X. J.; Li, C. S.; Cui, M. Y.; Song, Z. W.; Bai, X. Q.; Liang, C. W.; Wang, H. Y.; Zhang, T. Y. Synthesis, biological evaluation of benzothiazole derivatives bearing a 1,3,4-oxadiazole moiety as potential anti-oxidant and anti-inflammatory agents. *Bioorg. Med. Chem. Lett.* **2020**, 30, 127237.

(13) Chen, T. B.; Wu, Y. Y. Research progress of oxadiazole electron transport materials. *New Chem. Mater*. **2009**, 37, 15–17.

(14) Zhang, Z. M.; Li, G. W.; Ma, Y. G.; Wu, F.; Tian, W. J.; Shen, J. C. Synthesis of oxadiazole derivatives containing thiophene ring as electron transport materials in OEL devices. *Chin. J. Org. Chem.* **2000**, 20, 529–532.

(15) Li, Y.; Liu, J.; Zhang, H. Q.; Yang, X. P.; Liu, Z. J. Stereoselective synthesis and fungicidal activities of (*E*)-*α*-(methoxyimino)-benzeneacetate derivatives containing 1,3,4-oxadiazole ring. *Bioorg. Med. Chem. Lett.* **2006**, 16, 2278−2282.

(16) Li, P.; Yin, J.; Xu, W. M.; Wu, J.; He, M.; Hu, D. Y.; Yang, S.; Song, B. A. Synthesis, antibacterial activities, and 3*D*-QSAR of sulfone derivatives containing 1,3,4-oxadiazole moiety. *Chem. Biol. Drug Des.* **2013**, 82, 546−556.

(17) Li, P.; Shi, L.; Yang, X.; Yang, L.; Chen, X. W.; Wu, F.; Shi, Q. C.; Xu, W. M.; He, M.; Hu, D. Y.; Song, B. A. Design, synthesis, and antibacterial activity against rice bacterial leaf blight and leaf streak of 2,5-substituted-1,3,4-oxadiazole/thiadiazole sulfone derivative. *Bioorg. Med. Chem. Lett.* **2014**, 24, 1677−1680.

(18) Su, S. H.; Zhou, X.; Liao, G. P.; Qi, P. Y.; Jin, L. H. Synthesis and antibacterial evaluation of new sulfone derivatives containing 2-aroxymethyl-1,3,4-oxadiazole/thiadiazole moiety. *Molecules* **2017**, 22, 64.

(19) Wang, S. B.; Gan, X. H.; Wang, Y. J.; Li, S. Y.; Yi, C. F.; Chen, J. X.; He, F. C.; Yang, Y. Y.; Hu, D. Y.; Song, B. A. Novel 1,3,4-oxadiazole derivatives containing a cinnamic acid moiety as potential bactericide for rice bacterial diseases. *Int. J. Mol. Sci.* **2019**, 20, 1020.

(20) Hu, A. X.; Li, K. M.; Xie, W. X.; Ye, J.; Chen, J.; Xie, B. J.; Ren, H. D. A preparation method of trifloxystrobin and its intermediate. CN 108863845 A. 2018−11−23.

(21) Zhu, Z. L.; Zhang, R. H.; Yuan, L. L.; Ni, Y. M. A method of preparing trifloxystrobin. CN 1560027 A. 2005−01−05.

(22) Zhang, R. H.; Zhu, Z. L.; Li, Y. J. A high-yield synthesis process of trifloxystrobin. CN 1793115 A. 2006−06−28.

(23) Wang, X. B.; Yan, J. H.; Wang, M. Q.; Liu, M. H.; Zhang, J. P.; Chen, L. J.; Xue, W. Synthesis and three-dimensional quantitative structure-activity relationship study of quinazoline derivatives containing a 1,3,4-oxadiazole moiety as efficient inhibitors against Xanthomonas axonopodis pv. citri. *Mol. Divers.* **2018**, 22, 791−802.

(24) Sheldrick, G. M. A short history of SHELXS. *Acta. Cryst.* **2008**, A64, 112−122.

(25) Sheldrick, G. M. *SHELXS-97, Program for X-ray Crystal Structure Solution*. University of Göttingen. Germany **1997**.

(26) Song, B. A.; Chen, Y. Z.; Chen, J. X.; Wang, Y. J.; Wang, Z. Z.; Zhou, D. G.; Gan, X. H. Styryl-containing 1,3,4-oxadiazole sulfide compound, preparation method and application thereof. CN 106674147 A. 2017−05−17.

(27) Liu, A. P.; Yu, W. Q.; Liu, M. H.; Bai, J. J.; Liu, W. D.; Liu, X. P.; Pei, H.; Hu, L.; Huang, M. Z.; Wang, X. G. Synthesis and insecticidal activity of novel nitropyridyl-based dichloropropene ethers. *J. Agric. Food Chem.* **2015**, 63, 7469−7475.

(28) Abu-Awwad, F.; Politzer, P. Variation of parameters in Becke-3 hybrid exchange correlation functional. *J. Comput. Chem*. **2015**, 21, 227−238.

(29) Lee, C.; Wang, W.; Parr, R. G. Development of the Colle-Salvetti correlation energy formula into a functional of the electron density. *Phys. Rev. B* **1988**, 37, 785−789.

(30) Lu, T.; Chen, F. W. Multiwfn: a multifunctional wavefunction analyzer. *J. Comput. Chem.* **2012**, 33, 580−592.

(31) Lu, T.; Chen, F. W. Quantitative analysis of molecular surface based on improved marching tetrahedra algorithm. *J. Mol. Graph. Model*. **2012**, 38, 314−323.

(32) Humphrey, W.; Dalke, A.; Schulten, K. VMD: visual molecular dynamics. *J. Mol*. *Graph*. **1996**, 14, 33−38.

(33) Guo, H.; Han, J.; Pang, M. L.; Ma, Y. X.; Meng, J. B. Synthesis and characterization of acrylate group bridged *γ*-substituted *β*-diketopyrazole and isoxazole derivatives. *Chem. J. Chinese Universities* **2005**, 26, 1845−1848.

(34) Zhang, Y.; Shi, W. F. Synthesis and photopolymerization properties of self-initiated photopolymerized acrylate oligomers. *Chem. J. Chinese Universities* **2012**, 33, 635−639.

(35) Xiao, J. C.; Wu, Q.; Lei, Y.; Sun, J. R.; Jiang, F.; Xu, Y.; Xu, X. D.; Li, T. Y. Synthesis, single-crystal X-ray structure, theoretical studies of triple-{Mn-III-Schiff-base}-decorated molybdate. *Crystals* **2019**, 9, 657.

(36) Janiak, C. A critical account on *π*-*π* stacking in metal complexes with aromatic nitrogen-containing ligands. *J. Chem. Soc., Dalton Trans*. **2000**, 21, 3885−3896.

(37) Wang, B. L.; Shi, Y. X.; Zhang, S. J.; Ma, Y.; Wang, H. X.; Zhang, L. Y.; Wei, W.; Liu, X. H.; Li, Y. H.; Li, Z. M.; Li, B. J. Syntheses, biological activities and SAR studies of novel carboxamide compounds containing piperazine and arylsulfonyl moieties. *Eur. J. Med. Chem.* **2016**, 117, 167−178.

(38) Karelson, M.; Lobanov, V. S. Quantum-chemical descriptors in QSAR/QSPR studies. *Chem. Rev*. **1996**, 96, 1027−1043.

(39) Farag, A. M.; Fahim, A. M. Synthesis, biological evaluation and DFT calculation of novel pyrazole and pyrimidine derivatives. *J. Mol. Struct.* **2019**, 1179, 304−314.

(40) Du, Q. S.; Wang, C. H.; Wang, Y. T.; Huang, R. B. Empirical and accurate method for the three dimensional electrostatic potential (EM-ESP) of biomolecules. *J. Phys. Chem. B* **2010**, 114, 4351−4357.

(41) Murray, J. S.; Politzer, P. The electrostatic potential: an overview. *Wires Comput. Mol. Sci*. **2011**, 1, 153−163.